COMPOSITION OF THE MARTIAN POLAR CAPS FROM RADAR, ELEVATION, AND GRAVITY DATA.
A. Broquet[1], M. A. Wieczorek[1], and W. Fa[2], [1]Observatoire de la Côte d'Azur, Laboratoire Lagrange, Université Côte d'Azur, Nice, France (adrien.broquet@oca.eu) [2]Institute of Remote Sensing and Geographical Information System, School of Earth and Space Sciences, Peking University, Beijing, China.

Introduction: The north and south polar caps of Mars are tremendous reservoirs of ices and dust of unknown composition [1]. Both polar caps are geologically young ($<$ 100 Ma [2]) and their stratigraphically layered deposits are a witness to the planet's recent climate evolution. They act as large scale loads that can bend the basement. Analysis of the associated lithospheric flexure gives access to the composition of the polar caps and to the present-day strength of the lithosphere, which is related to the thermal state of the planet [3].

In this study, we use a novel technique [4] that combines radar and elevation data with a flexure model to probe the basement of the Martian south and north polar caps and jointly invert for their composition and the strength of the underlying lithosphere.

Methods and Data: For each polar cap, we invert for the elastic thickness of the lithosphere (T_e), the polar cap load density (ρ), and the real part of the dielectric constant (ε), by minimizing the root-mean-square of the misfit between the thickness of the polar cap predicted by a flexure model and the thickness observed by sounding radar [4, 5]. The misfit function is

$$\psi(\varepsilon, T_e, \rho) = [h_e - h_0 - W(T_e, \rho)] - h_t(\varepsilon), \qquad (1)$$

where h_e is surface elevation, h_0 is an estimated pre-loading surface topography, W is the computed deflection of the polar cap basement, and h_t is the thickness of the polar cap derived from radar data [4]. All terms depend implicitly on position.

h_0 is estimated using surface elevation data exterior to the polar cap and interpolating poleward using a minimum curvature method [6]. The uncertainty associated with this method is assessed by comparing h_0, obtained using various masking procedures and interpolation parameters [4]. h_t is obtained at several locations by investigating all nearby available radargrams from MARSIS (Mars Advanced Radar for Subsurface and Ionosphere Sounding) data, and identifying visually the reflections arising from the icy surface and the ice/substratum interface. We use data from several orbital tracks and ensure that the selected echoes are laterally continuous at a scale larger than the Fresnel zone of MARSIS. This allows to avoid interpreting off-nadir echoes as surface echoes, and spurious subcrustal reflectors as the polar cap basement.

For the south polar cap, we determined h_t at 1000 locations (Figure 1, right), and the obtained radar thicknesses are consistent with [7]. In regions colored in grey

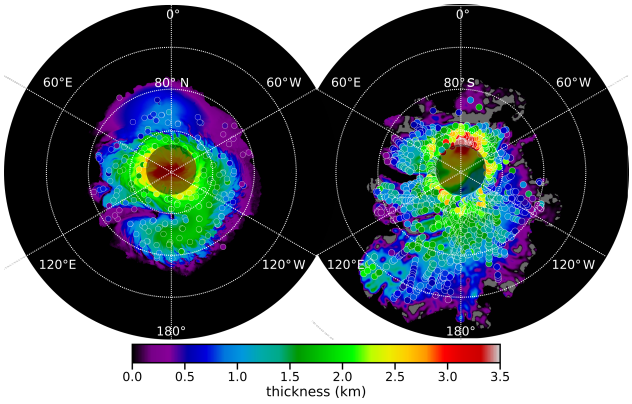

Figure 1: Estimated thickness of the north (left) and south (right) polar caps from surface elevations under the assumption that the base of the cap follows the regional slope (map), and radar data assuming $\varepsilon = 3$ (circle). Grey colors in the map indicate negative thicknesses.

of Figure 1, the predicted thickness of the polar deposits based on elevation data is negative, which is due to the elevation of the interpolated pre-loading basement exceeding the elevation of the deposits locally. This has no influence on the forthcoming results. Following [8], gravity and topography data are also used to give bounds on the allowed T_e and ρ. This procedure involves matching the spectral ratio of the gravity and topography (i.e., the admittance) to a theoretical loading model [8].

For the north polar cap, h_t was estimated at 213 locations (Figure 1, left), and the results are consistent with [9]. At the north pole, the gravity field is not used as there are important signals originating from subsurface loads that have no surface expressions [10].

Results: The inversion results for the polar caps are shown in Figure 2. The black lines and fill give a contour of the maximum allowed misfit of eq. 1, where the range of ε and ρ were limited such that they can be simultaneously obtained by mixtures of ices and dust. The green line limits the parameter space of the south pole to possible mixtures that fit the ranges of T_e and ρ given by an admittance analysis [8].

In this plot, the maximum allowed misfits were set to 412 m and 266 m for the south and north polar caps, respectively. These include uncertainties from the range resolution of MARSIS (86.5 m for both), surface roughness at the scale of the Fresnel zone of MARSIS (200 and 185 m), and that in the estimation of h_0 (350 and 170 m).

To determine plausible mixtures of ices and dust, the dielectric constant of solid CO_2, H_2O ice, and dust were set to 2.2, 3 (and 3.15) and 6 (and 8.8) respectively, and the densities of solid CO_2 and H_2O ice were assumed to be 1560 and 920 kg m^{-3}. The density of the dust component was allowed to vary from 2200 to 3400 kg m^{-3}, which covers the range from gypsum to basalt [11].

We further note that the thermal conductivity of the polar cap is strongly dependent on the relative abundances of ices and dust [8]. If the effective thermal conductivity is low enough, this could result in temperatures that would be sufficient to melt CO_2 ice at the base of the cap. Because basal melting has not yet been unequivocally observed by radar sounders, the black lines only show compositions that do not produce basal melting for a typical heat flow of 25 mW m^{-2} [3].

For the south polar cap and without gravity constraints, we observe that ε varies from 2.6 to 3.9, T_e is greater than 90 km, and ρ is less than 1960 kg m^{-3}. With gravity constraints, ε is 2.6 to 3.5, T_e is at least 150 km, and ρ is allowed to vary from 1100 to 1300 kg m^{-3}. For the north polar cap, ε can range from 2.6 to 3.1, T_e is at least 330 km, and ρ is at most 1440 kg m^{-3}.

In Figure 3, we show an example ternary diagram for the composition (in vol%) of the south (dashed) and north (solid) polar caps that fit our constraints on ρ and ε, under the assumption that both are made of dust, H_2O and CO_2 ices. We observe a strong trade-off between the allowed quantity of dust and dry ice. The north and south poles have dust contents less than 28% and 22%, and dry ice contents of at most 68 and 60%, respectively. Having less than 5% of dust within the north polar cap is inconsistent with the results of [11]. For a dust content of 6%, the north polar cap is required to have at least 8% dry ice, which is about 9 times larger than the massive CO_2 packs found at the south pole by [1]. Assuming a dust content of 6% for the south polar cap, the CO_2 content is 5%, 8 times larger than found in [1].

Discussion and Conclusion: Using the formalism of [12], the minimum T_e at the south and north pole imply heat flows of 26 and 16 mW m^{-2}, respectively, which are consistent with [3]. The north polar value is significantly different from that found in [13] (12 mW m^{-2}), which is largely the result of their having mistook previously reported relative deflections between two points with the maximum absolute deflection in the center of the deposit [see 4].

For both polar caps, we observe a trade-off between the dust and dry ice component. The inferred composition of the north polar cap implies that there must be at least 8% solid CO_2 mixed within the cap. Adding some dust would require an even larger solid CO_2 content. Assuming a reasonable dust content of 6% within the south pole gives a CO_2 content of 5%, 8 times larger than found in [1]. This represents a significant quantity of trapped volatiles that must be accounted for when establishing the inventory of available volatile reservoirs on Mars.

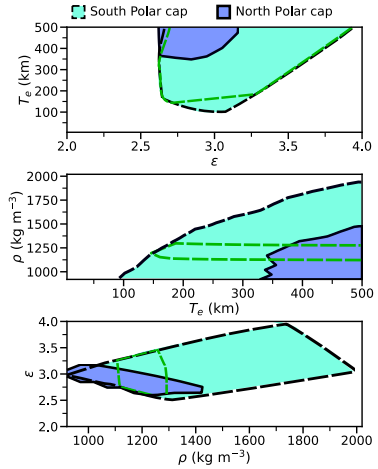

Figure 2: Inversion results for the polar caps. The black lines delimit possible mixtures that do not produce basal melting for a heat flow of 25 mW m^{-2}. The green line limits the parameter space of the south pole to mixtures fitting the ranges of T_e and ρ given by our admittance analysis.

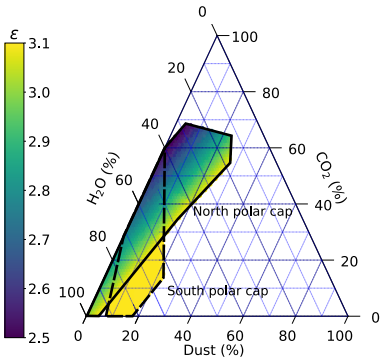

Figure 3: Ternary diagrams for the composition (in vol%) of the north (solid) and south (dashed) polar caps based on the constraints on ρ and ε.

References: [1] Phillips R. J. et al. (2011) *Science, 332*, 838–841. [2] Herkenhoff K. E. and Plaut J. J. (2000) *Icarus, 144*, 243–253. [3] Plesa A.-C. et al. (2018) *GRL, 45*, 12,198–12,209. [4] Broquet A. et al. (2020) *GRL, 47*. [5] Broquet A. and Wieczorek M. A. (2020) *Submitted to JGR*. [6] Smith W. H. F. and Wessel P. (1990) *Geophysics, 55*, 293–305. [7] Plaut J. J. et al. (2007) *Science, 316*, 92–95. [8] Wieczorek M. A. (2008) *Icarus, 196*, 506–517. [9] Grima C. et al. (2009) *GRL, 36*. [10] Ding M. et al. (2019) *JGR, 124*, 3095–3118. [11] McNutt M. K. (1984) *JGR, 89*, 180–194. [12] Ojha L. et al. (2019) *GRL, 46*, 12756–12763.